Nearly free-photon approximation for two-dimensional photonic crystal slabs

T. Ochiai[1] and K. Sakoda[2]
[1]*Departamento de Física Teórica de la Materia Condensada, Facultad de Ciencias, Universidad Autónoma de Madrid, Madrid 28049, Spain*
[2]*Research Institute for Electronic Science, Hokkaido University, Sapporo 060-0812, Japan*
(Received 25 January 2001; published 2 July 2001)

The nearly free-photon approximation for two-dimensional photonic crystal slabs is investigated. Diffraction loss and mixing of different polarizations in the photonic crystal slabs are quantitatively estimated. The selection rules among irreducible representations of k groups are shown to be essential in these phenomena. Numerical calculations in terms of the finite-difference time-domain method for a photonic crystal slab with a weak periodic modulation show good agreement with the results of the nearly free-photon approximation.

DOI: 10.1103/PhysRevB.64.045108 PACS number(s): 02.20.−a, 41.20.Jb, 42.70.Qs, 42.82.Et

I. INTRODUCTION

Since Yablonovitch[1] and John[2] suggested the possibility of controlling the radiation field and the optical properties of matter in photonic crystals, they have been one of the major subjects of research in physics and optoelectronics. Among the various kinds of photonic crystal, one-dimensional ones have a long history,[3] realizing fruitful technological applications. Two-dimensional photonic crystals were experimentally realized and their properties studied thoroughly in the last decade. However, the most promising three-dimensional photonic crystals are difficult to fabricate although their properties have been investigated by theoretical studies. Their fabrication and experimental studies on their basic properties have recently become major subjects of research. The properties of these photonic crystals can be understood by analogy with Bloch electrons in ordinary crystals, taking account of the vector nature of the Maxwell equations and of the Bose statistics of photons.

Recently, a combined structure of a thin dielectric slab and a two-dimensional photonic crystal, named a photonic crystal slab, has attracted much attention as an alternative to the three-dimensional photonic crystal.[4–18] Instead of achieving a complete photonic band gap, the photonic crystal slab uses index guiding in the vertical direction and a two-dimensional photonic band gap as a mechanism of three-dimensional photon confinement. Since electro-magnetic properties, e.g., the existence of the light line appear strongly in photonic crystal slabs, the simple analogy to Bloch electrons cannot be applied. This circumstance makes it difficult to study their properties theoretically. Most theoretical studies depend on numerical tasks like the finite-difference time-domain (FDTD) method,[9,11,12,17] the plane wave expansion method,[13,18] and diagonalization in the coupled mode approximation.[16] However, it is generally believed that analytical studies based on some approximations are helpful to understand physical properties.

In this paper we apply the nearly free-photon approximation[2,19] to photonic crystal slabs. This approximation is the photonic counterpart of the nearly free-electron approximation[20] for Bloch electrons. As we will see, it is possible to understand how the diffraction loss and the mixing of modes with different polarizations, which are remarkable features of photonic crystal slabs, occur in this approximation. In addition, the approximation predicts the band gap width, irreducible representations, and so on. The results of our recent studies on a photonic crystal slab with a strong periodic modulation[21] are quantitatively not far from the results of this approximation. Thus, this approximation is expected to be widely applicable.

The paper is organized as follows. In Sec. II we briefly summarize the degenerate perturbation theory for the Maxwell equations. In Sec. III the properties of symmetric dielectric slabs are given as the zeroth order approximation of photonic crystal slabs. The nearly free-photon approximation is investigated for photonic crystal slabs in Sec. IV. The real and imaginary parts of the eigenfrequencies are calculated for high symmetry points in the first Brillouin zone. In Sec. V numerical calculations are performed using both the FDTD method and the nearly free-photon approximation. The results obtained by the nearly free-photon approximation and by numerical calculations using the FDTD method are compared in the case of a photonic crystal slab with a weak periodic modulation. In Sec. VI we summarize our results.

II. DEGENERATE PERTURBATION THEORY FOR THE MAXWELL EQUATIONS

Maxwell's wave equation in a spatially modulated medium can be written as

$$\nabla\times\left(\frac{1}{\epsilon_r(\mathbf{x})}\nabla\times\mathbf{H}(\mathbf{x})\right)=\frac{\Omega^2}{c^2}\mathbf{H}(\mathbf{x}), \tag{1}$$

for a magnetic field in a stationary state. Here, $\epsilon_r(\mathbf{x})$ is the relative permittivity of the medium, c is the light velocity in vacuum, and Ω is the eigenfrequency of the state. The relative permeability was set to unity. We assume that the inverse of the relative permittivity can be split into two parts as

$$\frac{1}{\epsilon_r(\mathbf{x})}=\frac{1}{\epsilon_{\mathrm{un}}(\mathbf{x})}+\frac{1}{\epsilon_{\mathrm{pe}}(\mathbf{x})}, \tag{2}$$

where $\epsilon_{\mathrm{pe}}(\mathbf{x})$ describes a weak perturbation from an unperturbed system whose relative permittivity is given by $\epsilon_{\mathrm{un}}(\mathbf{x})$. The unperturbed system is assumed to be exactly solved. In

the perturbation treatment for the wave equation the magnetic field and the square of the eigenfrequency Ω^2 are expanded as

$$\mathbf{H}(\mathbf{x})=\mathbf{H}_0(\mathbf{x})+\mathbf{H}_1(\mathbf{x})+\mathbf{H}_2(\mathbf{x})+\cdots, \tag{3}$$

$$\Omega^2=\Omega_0^2+\Omega_1^2+\Omega_2^2+\cdots, \tag{4}$$

where $\mathbf{H}_i$ and Ω_i^2 are the ith order perturbations of the magnetic field and the square of the eigenfrequency, respectively. Then we solve the ith order Maxwell equation in turn.

Since the solutions of the zeroth order equation except for the longitudinal modes form a complete set of the transverse wave, $\mathbf{H}_i(\mathbf{x})$ $(i=1,2,\ldots,)$ can be expanded as a complete set. We assume that there is n-fold degeneracy in the zeroth order equation,

$$\nabla\times\left(\frac{1}{\epsilon_{\mathrm{un}}(\mathbf{x})}\nabla\times\mathbf{h}_{0\alpha}(\mathbf{x})\right)=\frac{\omega_0^2}{c^2}\mathbf{h}_{0\alpha}(\mathbf{x}) \quad (\alpha=1,\ldots,n),$$
$$\nabla\times\left(\frac{1}{\epsilon_{\mathrm{un}}(\mathbf{x})}\nabla\times\mathbf{h}_{i}(\mathbf{x})\right)=\frac{\omega_i^2}{c^2}\mathbf{h}_{i}(\mathbf{x}) \quad (i=1,2,\ldots), \tag{5}$$

where $\omega_i\neq\omega_0$ (for $i\neq 0$). The set $\{\mathbf{h}_I\}$ is orthonormalized as

$$\int d^3x\mathbf{h}_I^*\cdot\mathbf{h}_J=\delta_{IJ}. \tag{6}$$

Let us consider the case where the state concerned in the zeroth order approximation is degenerate. In accordance with the degenerate perturbation theory in quantum mechanics, $\mathbf{H}_0(\mathbf{x})$ is expanded in degenerate states as

$$\mathbf{H}_0(\mathbf{x})=\sum_{\alpha=1}^{n}a_\alpha^{(0)}\mathbf{h}_{0\alpha}. \tag{7}$$

If the degeneracy is lifted in the first order perturbation, the coefficient $a_\alpha^{(0)}$ and Ω_1 are determined by solving the following eigenvalue equation:

$$\sum_{\beta=1}^{n}M_{(0\alpha)(0\beta)}a_\beta^{(0)}=\frac{\Omega_1^2}{c^2}a_\alpha^{(0)} \quad (\alpha=1,\ldots,n), \tag{8}$$

where

$$M_{IJ}=\int d^3x\mathbf{h}_I^*(\mathbf{x})\cdot\nabla\times\left(\frac{1}{\epsilon_{\mathrm{pe}}(\mathbf{x})}\nabla\times\mathbf{h}_J(\mathbf{x})\right)$$
$$=\omega_I\omega_J\epsilon_0^2\int d^3x\frac{1}{\epsilon_{\mathrm{pe}}(\mathbf{x})}\epsilon_{\mathrm{un}}^2(\mathbf{x})\mathbf{e}_I^*(\mathbf{x})\cdot\mathbf{e}_J(\mathbf{x}), \tag{9}$$

and

$$\nabla\times\mathbf{h}_I(\mathbf{x})=-i\omega_I\epsilon_0\epsilon_{\mathrm{un}}(\mathbf{x})\mathbf{e}_I(\mathbf{x}). \tag{10}$$

Here, the surface term appearing in the partial integral of Eq. (9) is assumed to vanish. The second order perturbation for the lifted mode gives the following correction to its eigenfrequency:

$$\frac{\Omega_2^2}{c^2}=-\sum_{i,\alpha,\beta}\frac{a_{0\alpha}^{(0)*}M_{(0\alpha)i}M_{i(0\beta)}a_{0\beta}^{(0)}}{\omega_i^2/c^2-\omega_0^2/c^2}, \tag{11}$$

where $\mathbf{H}_0$ is normalized as $\int d^3x\mathbf{H}_0^*\cdot\mathbf{H}_0=1$. Thus, the modes with higher frequency than ω_0 in the zeroth order equation always give negative corrections to the eigenfrequency.

III. PROPERTIES OF SYMMETRIC DIELECTRIC SLABS

As is well known, a dielectric slab sandwiched by materials with lower dielectric constants serves as a planar waveguide for electromagnetic waves. An electromagnetic wave under certain conditions, given below is guided in the slab owing to total internal reflection. If the slab is thin enough, a single guided mode is realized. While the electromagnetic properties of the dielectric slab are known well, we present them in order to make the paper self-contained.

We assume that the slab with dielectric constant ϵ_2 and thickness d is sandwiched by a material with dielectric constant ϵ_1 and thickness L. The thickness L is large compared with d. We also assume that the slab has infinite extent in the plane. In this case, owing to the translational invariance in the plane, each eigenmode is characterized by an in-plane wave vector $\mathbf{k}_p$. If the frequency ω of the electromagnetic wave is less than $c|\mathbf{k}_p|/\sqrt{\epsilon_1}$, the wave is guided in the slab. The guided mode has a discrete spectrum and thus the spectrum forms a band structure below the light line, which is defined by $\omega=c|\mathbf{k}_p|/\sqrt{\epsilon_1}$. On the other hand, if $\omega>c|\mathbf{k}_p|/\sqrt{\epsilon_1}$, the electromagnetic wave is radiated away from the slab. The radiation mode has a continuum spectrum above the light line.

The guided and radiation modes are classified according to their polarizations (TE or TM). In the TE (TM) polarization, the polarization vector of the electric (magnetic) field lies in plane and is perpendicular to the in-plane wave vector $\mathbf{k}_p$. However, there is an exception at $\mathbf{k}_p=\mathbf{0}$. The radiation modes with $\mathbf{k}_p=\mathbf{0}$ are both TE and TM polarized, so we must work carefully at this point.

Since there is a mirror symmetry in the direction perpendicular to the plane, the eigenmodes are further classified according to the parity σ_z of the mirror symmetry. If $\sigma_z=1$ (-1), the field profile of the in-plane component of the electric field is symmetric (antisymmetric) with respect to the plane bisecting the slab vertically. In what follows, we concentrate on the modes with $\sigma_z=1$. The modes with $\sigma_z=-1$ can be treated in a similar manner. The discrete spectrum of the guided modes with $\sigma_z=1$ is given by solving the following equations:

$$\kappa_1\cos\left(\frac{k_2d}{2}\right)-k_2\sin\left(\frac{k_2d}{2}\right)=0, \quad (\mathrm{TE}), \tag{12}$$

$$\epsilon_2\kappa_1\sin\left(\frac{k_2d}{2}\right)+\epsilon_1k_2\cos\left(\frac{k_2d}{2}\right)=0, \quad (\mathrm{TM}), \tag{13}$$

where

$$\kappa_1 = \sqrt{\mathbf{k}_p^2 - \epsilon_1 \frac{\omega^2}{c^2}},$$

$$k_2 = \sqrt{\epsilon_2 \frac{\omega^2}{c^2} - \mathbf{k}_p^2}. \tag{14}$$

We should note that there is an infrared cutoff for the modes with TM polarization. The cutoff frequency is given by

$$\omega_c = \frac{\pi c}{d\sqrt{\epsilon_2 - \epsilon_1}}. \tag{15}$$

A single mode of TE polarization is realized below the cutoff. Even if a weak perturbation of the periodic modulation is added, guided modes below the cutoff are almost TE polarized.

The field profile of the guided modes is given by

$$\mathbf{E}^g_{\mathrm{TE}} = \frac{(\hat{\mathbf{k}}_p \times \hat{z}) e^{i\mathbf{k}_p \cdot \mathbf{x}_p}}{\sqrt{N^g_{\mathrm{TE}}(\omega, \mathbf{k}_p)}} \times \begin{cases} \cos(k_2 z) & \text{for } 0 < z < d/2 \\ e^{-\kappa_1 (z - d/2)} \cos(k_2 d/2) & \text{for } z > d/2, \end{cases} \tag{16}$$

$$N^g_{\mathrm{TE}}(\omega, \mathbf{k}_p) = \frac{2S}{\mu_0^2 \omega^2} \left[\frac{\mathbf{k}_p^2 - k_2^2}{4k_2} \sin(k_2 d) + \frac{d}{4}(\mathbf{k}_p^2 + k_2^2) + \frac{\mathbf{k}_p^2 + \kappa_1^2}{2\kappa_1} \cos^2\left(\frac{k_2 d}{2}\right) \right] \tag{17}$$

for TE polarization and

$$\mathbf{H}^g_{\mathrm{TM}} = \frac{(\hat{\mathbf{k}}_p \times \hat{z}) e^{i\mathbf{k}_p \cdot \mathbf{x}_p}}{\sqrt{N^g_{\mathrm{TM}}(\omega, \mathbf{k}_p)}} \times \begin{cases} \sin(k_2 z) & \text{for } 0 < z < d/2 \\ e^{-\kappa_1 (z - d/2)} \sin(k_2 d/2) & \text{for } z > d/2, \end{cases} \tag{18}$$

$$N^g_{\mathrm{TM}}(\omega, \mathbf{k}_p) = 2S \left[\frac{d}{4} - \frac{1}{4k_2} \sin(k_2 d) + \frac{1}{2\kappa_1} \sin^2\left(\frac{k_2 d}{2}\right) \right] \tag{19}$$

for TM polarization. Here, $\hat{\mathbf{k}}_p$ is the unit vector with the same direction as $\mathbf{k}_p$ and S is the area of the plane which is supposed to be infinite. The normalization factors N^g were determined by requiring the inner product $\int d^3x \mathbf{H}^*(\mathbf{x}) \cdot \mathbf{H}(\mathbf{x})$ to be unity. The field profiles at negative z can be obtained by parity transformation as $E_x(z) = \sigma_z E_x(-z)$, etc. The guided modes are evanescent outside the slab. Thus, the Poynting vector of the guided mode does not have a vertical component and is proportional to $\mathbf{k}_p$.

The field profile of the radiation mode is given by

$$\mathbf{E}^r_{\mathrm{TE}} = \frac{(\hat{\mathbf{k}}_p \times \hat{z}) e^{i\mathbf{k}_p \cdot \mathbf{x}_p}}{\sqrt{N^r_{\mathrm{TE}}(\omega, \mathbf{k}_p)}} \begin{cases} \cos(k_2 z) & \text{for } 0 < z < d/2 \\ \mathrm{Re}(A_{\mathrm{TE}} e^{ik_1 z}) & \text{for } z > d/2, \end{cases} \tag{20}$$

$$A_{\mathrm{TE}} = e^{-ik_1 d/2} \left[\cos\left(\frac{k_2 d}{2}\right) + i \frac{k_2}{k_1} \sin\left(\frac{k_2 d}{2}\right) \right],$$

$$N^r_{\mathrm{TE}}(\omega, \mathbf{k}_p) = |A_{\mathrm{TE}}|^2 SL \frac{\epsilon_0 \epsilon_1}{\mu_0} \tag{21}$$

for TE polarization and

$$\mathbf{H}^r_{\mathrm{TM}} = \frac{(\hat{\mathbf{k}}_p \times \hat{z}) e^{i\mathbf{k}_p \cdot \mathbf{x}_p}}{\sqrt{N^r_{\mathrm{TM}}(\omega, \mathbf{k}_p)}} \begin{cases} \sin(k_2 z) & \text{for } 0 < z < d/2 \\ \mathrm{Re}(A_{\mathrm{TM}} e^{ik_1 z}) & \text{for } z > d/2, \end{cases} \tag{22}$$

$$A_{\mathrm{TM}} = e^{-ik_1 d/2} \left[\sin\left(\frac{k_2 d}{2}\right) - i \frac{k_2}{k_1} \cos\left(\frac{k_2 d}{2}\right) \right],$$

$$N^r_{\mathrm{TM}}(\omega, \mathbf{k}_p) = |A_{\mathrm{TM}}|^2 SL \tag{23}$$

for TM polarization. Here, k_1 is given by

$$k_1 = \sqrt{\epsilon_1 \frac{\omega^2}{c^2} - \mathbf{k}_p^2}. \tag{24}$$

The same normalization prescription as for the guided mode is used. We reserved only the term proportional to L in the normalization factors. Since we consider the case where the upper and lower material with dielectric constant ϵ_1 can be regarded as having infinite thickness, we take the limit $L \to \infty$ finally. We should note that the radiation modes in $z > d/2$ have both incoming and outgoing waves in the vertical direction. This property is not appropriate when the diffraction loss in a photonic crystal slab is considered. We will present a prescription to avoid this problem in the next section.

It is interesting to make clear the state density of the radiation modes. Since the wave vector in plane is conserved, it is natural to define the state density with fixed $\mathbf{k}_p$. The state density $\rho(\omega, \mathbf{k}_p)$ is defined above the light line and is given by

$$\rho(\omega, \mathbf{k}_p) = \frac{1}{\pi} \frac{(\epsilon_1/c^2)\omega}{\sqrt{(\epsilon_1/c^2)\omega^2 - \mathbf{k}_p^2}} = \frac{\epsilon_1 \omega}{\pi c^2 k_1} \tag{25}$$

for each polarization. The total number of radiation modes with $\mathbf{k}_p$ is $L \int d\omega \rho(\omega, \mathbf{k}_p)$ for each polarization. The state density has divergence on the light path. As we will see, this is one of the crucial points for diffraction loss in a photonic crystal slab.

IV. NEARLY FREE-PHOTON APPROXIMATION

In this section, we investigate the nearly free-photon approximation for a photonic crystal slab. We regard the periodic modulation of the dielectric function in the photonic crystal slab as a perturbation. Then the eigenmodes in the dielectric slab discussed in the previous section are treated as the zeroth order approximation of the eigenmodes in the photonic crystal slab. The periodic modulation causes a reduction of the momentum space in plane in the first Brillouin zone. Thus band folding takes place for the guided modes.

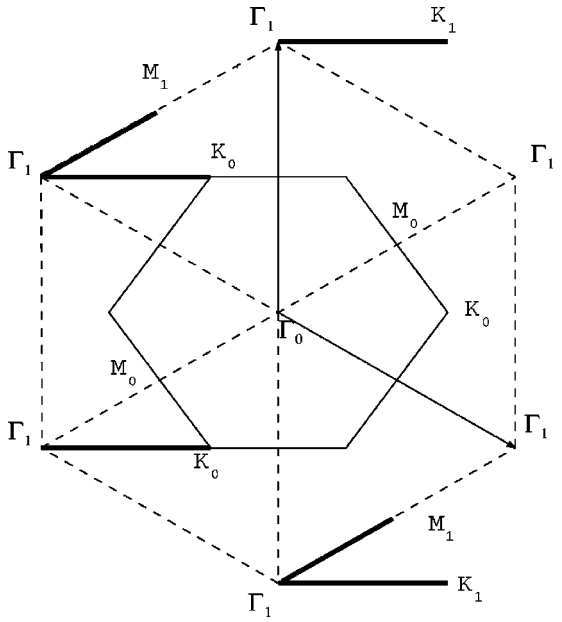

FIG. 1. The reciprocal lattice space for the hexagonal lattice. The bold lines between the high symmetry points Γ, M, and K are on the Bragg planes.

This causes three kinds of degeneracy in the zeroth order approximation.

The first kind of degeneracy occurs on the Bragg planes, as in the nearly free-electron approximation for Bloch electrons. This kind of degeneracy is generally lifted by the higher order perturbations and the lifting becomes the seed of a photonic band gap. The second kind of degeneracy occurs at an intersection point of TE and TM guided mode bands. This causes a mixing of TE and TM polarizations, which is absent in the two-dimensional photonic crystal with infinite height. The third kind of degeneracy occurs above the light line; that is, the degeneracy between the folded bands of the guided modes and the radiation modes. Generally, degeneracy between a state with a continuum spectrum and a state with a discrete spectrum does not occur for real eigenstates in quantum mechanics. In fact a state with a discrete spectrum in a band becomes a resonance state. This is the case for photonic crystal slabs. However, in the zeroth order approximation of photonic crystal slabs the degeneracy occurs in a distinct manner. This causes a singular perturbation of the guided modes and they become leaky. The latter two kinds of degeneracy are remarkable features of photonic crystal slabs.

In what follows, we restrict ourselves to the lifting of the degeneracies of the guided modes in the photonic crystal slab. The photonic crystal slab is supposed to have the periodicity of the hexagonal lattice and to be symmetric under mirror reflection with respect to the vertical direction. The reciprocal lattice space is shown in Fig. 1. The high symmetry points $\Gamma, M,$ and K are denoted with a subscript classifying the symmetry points according to the distance from the origin (Γ_0). The bold lines are on the Bragg planes. Among points with the same character, higher order degeneracies occur.

The band structure of guided modes in a photonic crystal slab with infinitely small periodic modulation (the empty lattice) is shown in Fig. 2. Here we assume that the thickness d of the slab is half of the lattice constant a and that the dielectric constant ϵ_2 of the slab is $(3.4)^2$. The slab is sandwiched by air ($\epsilon_1=1.0$). In Fig. 2 only the dispersion curves of the guided modes with $\sigma_z=1$ are shown. In this case intersections of the dispersion curves with different polarizations occurs both above and below the light line. As soon as the periodic modulation is added, the guided modes above the light line begin to mix with the radiation modes and thus become leaky.

Since we are concerned with the nearly free-photon approximation, the periodic modulation should be weak. As a weak perturbation, we consider a hexagonal array of dielectric cylinders with dielectric constant ϵ_{rod} fabricated in the dielectric slab as depicted in Fig. 3. In this case the perturbative part of the inverse dielectric function is given by

$$\frac{1}{\epsilon_{\mathrm{pe}}(\mathbf{x})}=\theta\left(\frac{d}{2}-z\right)\theta\left(z+\frac{d}{2}\right)\sum_{\mathbf{G}} U_{\mathbf{G}}\exp(i\mathbf{G}\cdot\mathbf{x}_p), \quad (26)$$

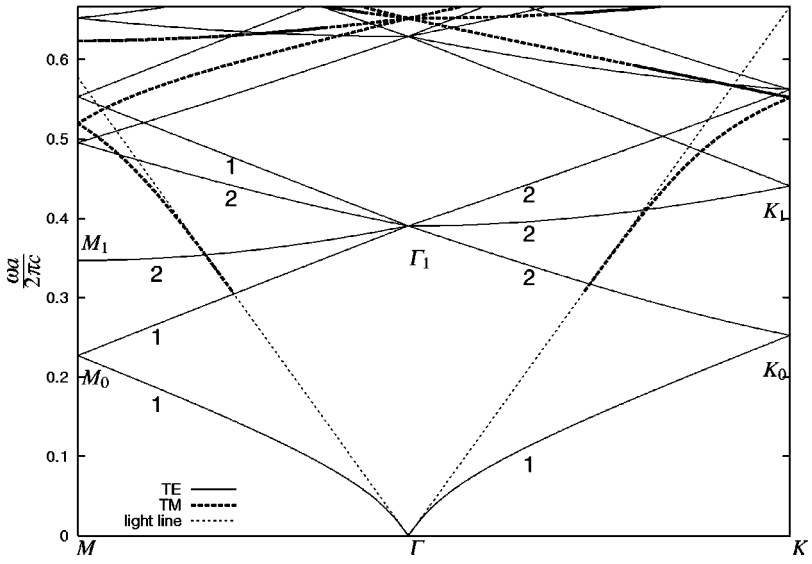

FIG. 2. The photonic band structure of guided modes in a dielectric slab with $\epsilon_1=1.0$, $\epsilon_2=(3.4)^2$. The band structure is shown in terms of the reduced zone scheme of the hexagonal lattice, where the thickness d of the slab is assumed to be half of the lattice constant a. The solid lines correspond to the TE guided modes and the bold dashed lines correspond to TM guided modes. The numbers attached below the bands indicate the degrees of degeneracy of the bands.

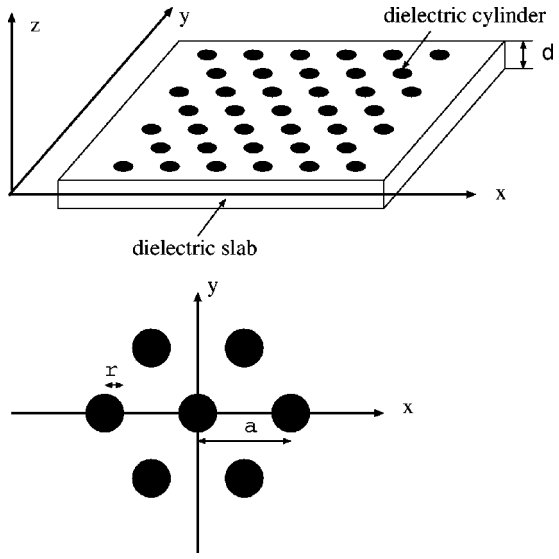

FIG. 3. Schematic illustration of the two-dimensional photonic crystal slab. It is composed of a regular hexagonal array of dielectric cylinders with dielectric constant $\epsilon_{\rm rod}$ fabricated in a dielectric slab with dielectric constant ϵ_2. The slab is sandwiched by a material with dielectric constant ϵ_1 in the z direction.

$$U_{\mathbf{G}}=\left(\frac{1}{\epsilon_{\rm rod}}-\frac{1}{\epsilon_2}\right)\frac{4\pi r}{\sqrt{3}a^2}\frac{J_1(|\mathbf{G}|r)}{|\mathbf{G}|}, \tag{27}$$

where $\mathbf{G}$ is the reciprocal lattice vector of the hexagonal lattice, that is, $\mathbf{G}_{n,m}=(n,(2m-n)/\sqrt{3})$ in units of $2\pi/a$, and $J_1(z)$ is the Bessel function of the first order. In order to justify the perturbative treatment, $\epsilon_{\rm rod}$ is assumed to be close to ϵ_2. The radius r of the dielectric cylinder is also assumed to be much less than the lattice constant a of the hexagonal lattice.

In the first order perturbation, the eigenfrequency of every mode is shifted owing to $U_{\mathbf{0}}$. Since $U_{\mathbf{0}}$ is given by the filling factor of the cylinders as

$$U_{\mathbf{0}}=\left(\frac{1}{\epsilon_{\rm rod}}-\frac{1}{\epsilon_2}\right)\frac{2\pi r^2}{\sqrt{3}a^2}, \tag{28}$$

it reduces or increases the spatially averaged dielectric constant of the slab depending on whether $\epsilon_{\rm rod}$ is smaller than ϵ_2 or not. However, the shifts in the eigenfrequencies are not straightforward. That is, in the first order approximation the shifted eigenfrequencies cannot be expressed as those in the dielectric slab with a spatially averaged dielectric constant. This is because the guided and radiation modes are not confined in the slab. This is also a remarkable feature of the photonic crystal slab.

Mixing of the guided modes and radiation modes does not occur in the first order perturbation. This is because the matrix elements M_{IJ} between the guided and radiation modes are suppressed on the order of the factor $1/\sqrt{L}$ coming from the normalization of the radiation modes. Thus, as far as the lifting of the degeneracy of the guided modes are concerned, we can neglect the contribution of the radiation modes. However, in the second order perturbation, the factor L appearing in the state density of the radiation modes cancels the suppression factor $1/L$ appearing in $|M_{IJ}|^2$ of Eq. (9). As we will see, this adds an imaginary part to the eigenfrequency of the leaky modes.

The matrix element M_{IJ} has much more information about the coupling among the eigenmodes, that is, the selection rule. Suppose that the set $\mathbf{e}_a^R(a=1,\ldots,\dim R)$ forms the basis of an irreducible representation R of the k group, that is,

$$\sum_{j=1}^{3}(G_{\mathbf{k}})_{ij}[\mathbf{e}_a^R(G_{\mathbf{k}}^{-1}x)]_j=\sum_{b=1}^{\dim R}D_{ab}^R(G_{\mathbf{k}})[\mathbf{e}_b^R(x)]_i. \tag{29}$$

Here, $G_{\mathbf{k}}$, is an element of the k group and $D^R(G_{\mathbf{k}})$ is its representation. Since $\epsilon_{\rm pe}$ has all symmetries of the k group, there is the selection rule

$$\int d^3x\frac{1}{\epsilon_{\rm pe}(x)}\mathbf{e}_a^R(x)\cdot\mathbf{e}_b^{R'}(x)=0 \quad \text{for } R\neq R'. \tag{30}$$

Thus, the matrix element M_{IJ} between modes with different irreducible representations is zero. As we will see, this causes interesting phenomena like stability at the Γ point. The selection rule is a key to understanding the physical properties of the photonic crystal slab.

A. The photonic band gap in the guided modes

As is well known, the TE-like modes (the modes with $\sigma_z=1$) in photonic crystal slabs with a hexagonal array of cylindrical air holes tend to have a photonic band gap below the light line. The gap usually appears between the first and second bands of the guided modes. The upper and lower band edges are at the M point of the second band and the K point of the first band, respectively. Since we consider the nearly free-photon approximation, strong periodic modulations which open a wide photonic band gap are beyond our scope. However, it is instructive to estimate the phase boundary between the gapless and gapfull phases in the first order perturbation of the nearly free-photon approximation. In order to do this we have to evaluate the eigenfrequencies at these points.

At the M_0 point there is a twofold degeneracy between the guided modes with $\mathbf{k}_p=\pm(1/2,1/(2\sqrt{3}))$ in unit of $2\pi/a$. These two vectors are separated by $\mathbf{G}_{1,1}$. This degeneracy is lifted in the first order perturbation owing to $U_{\mathbf{G}_{1,1}}$. The eigenvalue equation in the first order perturbation is given by

$$f(M_0)\begin{pmatrix}U_0 & -U_1\\ -U_1 & U_0\end{pmatrix}\begin{pmatrix}a_1^{(0)}\\ a_2^{(0)}\end{pmatrix}=\frac{\Omega_1^2}{c^2}\begin{pmatrix}a_1^{(0)}\\ a_2^{(0)}\end{pmatrix}, \tag{31}$$

where

$$f(\omega,\mathbf{k}_p)=\frac{2(\omega_0\epsilon_0\epsilon_2)^2S}{N_{\rm TE}(\omega,\mathbf{k}_p)}\left(\frac{d}{2}+\frac{\sin(k_2d)}{4k_2}\right) \tag{32}$$

and $U_1\equiv U_{\mathbf{G}_{1,1}}$. Since the k group at the M point is C_{2v}, the modes are classified by the irreducible representations of C_{2v}. The lifted modes have the A_2 and B_1 representation with

$$\frac{\Omega_1^2}{c^2}=f(M_0)(U_0-U_1),\quad \text{for } A_2,$$
$$\frac{\Omega_1^2}{c^2}=f(M_0)(U_0+U_1),\quad \text{for } B_1. \tag{33}$$

Since we consider a weak perturbation of the uniform slab, the radius should be small compared with the lattice constant. In this region $U_1>0$, so that the B_1 mode is higher in frequency than the A_2 mode.

On the other hand, at the K_0 point there is the threefold degeneracy among the guided modes with $\mathbf{k}_p=(2/3,0),(1/3,\pm 1/\sqrt{3})$ in units of $2\pi/a$. This degeneracy is partially lifted in the first order perturbation. The eigenvalue equation in the first order perturbation is given by

$$f(K_0)\begin{pmatrix} U_0 & -\frac{U_1}{2} & -\frac{U_1}{2} \\ -\frac{U_1}{2} & U_0 & -\frac{U_1}{2} \\ -\frac{U_1}{2} & -\frac{U_1}{2} & U_0 \end{pmatrix}\begin{pmatrix} a_1^{(0)} \\ a_2^{(0)} \\ a_3^{(0)} \end{pmatrix}=\frac{\Omega_1^2}{c^2}\begin{pmatrix} a_1^{(0)} \\ a_2^{(0)} \\ a_3^{(0)} \end{pmatrix}. \tag{34}$$

Since the k group at the K point is C_{3v}, the modes are classified by the irreducible representations of C_{3v}. The eigenvalue equation has a double root corresponding to the E representation and a single root with the A_2 representation. The eigenvalues are given by

$$\frac{\Omega_1^2}{c^2}=f(K_0)(U_0-U_1),\quad \text{for } A_2,$$
$$\frac{\Omega_1^2}{c^2}=f(K_0)\left(U_0+\frac{U_1}{2}\right),\quad \text{for } E. \tag{35}$$

The E mode is higher in frequency than A_2. Thus, a photonic band gap below the light path is possible if the frequency of the B_1 mode at M_0 is higher than that of the A_2 mode at K_0. We will see the phase diagram regarding the gap in Sec. V.

B. TE-TM mixing

In Fig. 2 we can see that extra degeneracies occur at the points where the folded bands of the TE and TM guided modes intersect. As a representative example, we study the TE-TM mixing in the Γ_1-K_0 interval. In this interval the k group consists of two elements $\{1,\sigma_y\}$, where σ_y is the parity transformation with respect to the y coordinate. Thus, the modes in Γ_1-K_0 are classified according to the eigenvalue of σ_y. Since there is a twofold degeneracy in the TE guided modes along Γ_1-K_0, we must diagonalize a 3×3 matrix at the intersection point:

$$\begin{pmatrix} M_e & M_{ee} & M_{em} \\ M_{ee} & M_e & -M_{em} \\ M_{em}^* & -M_{em}^* & M_m \end{pmatrix}\begin{pmatrix} a_1^{(0)} \\ a_2^{(0)} \\ a_3^{(0)} \end{pmatrix}=\frac{\Omega_1^2}{c^2}\begin{pmatrix} a_1^{(0)} \\ a_2^{(0)} \\ a_3^{(0)} \end{pmatrix}, \tag{36}$$

where

$$M_e=f(\mathbf{k}_p^*-\mathbf{G}_{1,0})U_0,$$
$$M_{ee}=f(\mathbf{k}_p^*-\mathbf{G}_{1,0})(\widehat{\mathbf{k}_p^*-\mathbf{G}}_{1,0}\cdot\widehat{\mathbf{k}_p^*-\mathbf{G}}_{1,1})U_1, \tag{37}$$
$$M_m=\frac{2S}{N_{\mathrm{TM}}(\omega,\mathbf{k}_p^*)}\left(\frac{d}{4}[(\mathbf{k}_p^*)^2+(k_2^{\mathrm{TM}})^2]-\frac{(\mathbf{k}_p^*)^2-(k_2^{\mathrm{TM}})^2}{4k_2^{\mathrm{TM}}}\sin(k_2^{\mathrm{TM}}d)\right)U_0, \tag{38}$$
$$M_{em}=i\frac{2S\omega_0\epsilon_0\epsilon_2(\widehat{\mathbf{k}_p^*-\mathbf{G}}_{1,0y}k_2^{\mathrm{TM}}}{\sqrt{N_{\mathrm{TE}}(\omega,\mathbf{k}_p^*-\mathbf{G}_{1,0})N_{\mathrm{TM}}(\omega,\mathbf{k}_p^*)}}\times\left(\frac{\sin[(k_2^{\mathrm{TM}}+k_2^{\mathrm{TE}})d/2]}{2(k_2^{\mathrm{TM}}+k_2^{\mathrm{TE}})}+\frac{\sin[(k_2^{\mathrm{TM}}-k_2^{\mathrm{TE}})d/2]}{2(k_2^{\mathrm{TM}}-k_2^{\mathrm{TE}})}\right)U_1.$$

Here, $\mathbf{k}_p^*$ is the wave vector at the intersection point reduced in the first Brillouin zone and

$$k_2^{\mathrm{TE}}=\sqrt{\epsilon_2\frac{\omega_0^2}{c^2}-(\mathbf{k}_p^*-\mathbf{G}_{1,0})^2},$$
$$k_2^{\mathrm{TM}}=\sqrt{\epsilon_2\frac{\omega_0^2}{c^2}-(\mathbf{k}_p^*)^2}. \tag{39}$$

The eigenvalues and parities are given by

$$\frac{\Omega_1^2}{c^2}=\begin{cases}\frac{1}{2}(M_m+M_e-M_{ee}\pm\sqrt{(M_m+M_e-M_{ee})^2+8|M_{em}|^2}), & \sigma_y=1\\ M_e+M_{ee}, & \sigma_y=-1.\end{cases} \tag{40}$$

The eigenvector with $\sigma_y=-1$ is purely TE polarized, that is, the TM component does not enter in the eigenvector. The other solutions with $\sigma_y=1$ are mixed states of TE and TM. We should note that on general points in the Γ_1-K_0 interval the degeneracy is lifted according to Eq. (36) in which the third row and column are neglected and $\mathbf{k}_p^*$ is replaced by a general point in this interval. In this case the shifts are given by

$$\frac{\Omega_1^2}{c^2}=\begin{cases} M_e-M_{ee}, & \sigma_y=1 \\ M_e+M_{ee} & \sigma_y=-1. \end{cases} \tag{41}$$

Thus, the intersection of the dispersion curves with TE and TM polarizations does not affect the mode with $\sigma_y=-1$. This is caused by symmetry mismatch between the lifted mode with $\sigma_y=-1$ and the TM guided mode. Since the TM guided mode has $\sigma_y=1$ in the Γ-K interval for low frequency, it does not couple with the modes with $\sigma_y=-1$. This phenomenon can be viewed as a consequence of the selection rule. The two degenerate guided modes with $\mathbf{k}_p^*-\mathbf{G}_{1,0}$ and $\mathbf{k}_p^*-\mathbf{G}_{1,1}$ of TE polarization can be regarded as linear combinations of two modes with $\sigma_y=\pm 1$. Then the matrix element between the mode with $\sigma_y=-1$ and the TM guided mode with $\mathbf{k}_p^*$ is zero owing to the selection rule. Thus, the mode with $\sigma_y=-1$ does not couple with the TM guided mode in the first order perturbation. The same phenomenon occurs at the intersection points in the Γ_1-K_1 interval. That is, the lifted modes with $\sigma_y=-1$ do not couple with the TM guided mode. Thus, this band is also almost TE polarized.

C. Stability at the Γ point

As we can see in Fig. 2, at the Γ_1 point six dispersion curves of the guided modes intersect each other in the band structure of the empty lattice. This is due to the degeneracy among the guided modes with in-plane wave vectors $\mathbf{k}_p=\mathbf{G}_{1,1},\mathbf{G}_{0,1},\mathbf{G}_{-1,0},\mathbf{G}_{-1,-1},\mathbf{G}_{0,-1},\mathbf{G}_{1,0}$. The degeneracy is partially lifted in the first order perturbation. To make certain of that, we must diagonalize the following 6×6 matrix:

$$f(\Gamma_1)\begin{pmatrix} U_0 & U_1/2 & -U_2/2 & -U_3 & -U_2/2 & U_1/2 \\ U_1/2 & -U_2/2 & -U_3 & -U_2/2 & U_1/2 & U_0 \\ -U_2/2 & -U_3 & -U_2/2 & U_1/2 & U_0 & U_1/2 \\ -U_3 & -U_2/2 & U_1/2 & U_0 & U_1/2 & -U_2/2 \\ -U_2/2 & U_1/2 & U_0 & U_1/2 & -U_2/2 & -U_3 \\ U_1/2 & U_0 & U_1/2 & -U_2/2 & -U_3 & -U_2/2 \end{pmatrix}, \tag{42}$$

where $U_2=U_{\mathbf{G}_{2,1}}$, $U_3=U_{\mathbf{G}_{0,2}}$. With the aid of group theory we can solve the eigenvalue equation immediately. As was noted in our previous paper,[21] the A_2, B_1, E_1, and E_2 representations of C_{6v}, which is the k group at the Γ point, are possible. We can construct these representations by linear combinations of the guided modes whose wave vectors are given above. It is easy to prove that these representations form the eigenvectors of the above matrix. As a result, the eigenfrequencies are given by

$$\frac{\Omega_1^2}{c^2}=f(\Gamma_1)(U_0+U_1-U_2-U_3), \quad \text{for } A_2,$$

$$\frac{\Omega_1^2}{c^2}=f(\Gamma_1)(U_0-U_1-U_2+U_3), \quad \text{for } B_1,$$

$$\frac{\Omega_1^2}{c^2}=f(\Gamma_1)\left(U_0+\frac{U_1}{2}+\frac{U_2}{2}+U_3\right), \quad \text{for } E_1,$$

$$\frac{\Omega_1^2}{c^2}=f(\Gamma_1)\left(U_0-\frac{U_1}{2}+\frac{U_2}{2}-U_3\right), \quad \text{for } E_2. \tag{43}$$

The Γ points are above the light line except for Γ_0. This seems to imply that the leaky modes readily decay into the radiation modes at these points. However, the selection rule forbids such a decay for the leaky modes with specific symmetries. That is, if there is no radiation mode with the matched representation, the decay into the radiation modes is forbidden. The radiation modes at the Γ point have only the E_1 representation for $\omega<2/\sqrt{3}$ in units of $2\pi c/a$.[21] Thus, the matrix elements M_{IJ} between the lifted modes with the A_2,B_1,E_2 representations and the radiation modes are zero. Thus, the A_2,B_1, and E_2 modes are stable against decay into the radiation modes.

D. Diffraction loss above the light line

Folding the bands of the guided modes into the first Brillouin zone inevitably causes a coupling with the radiation modes. As was mentioned, the coupling is suppressed on the order of $1/\sqrt{L}$ in the first order perturbation. The diffraction loss appears from the second order perturbation. In Sec. III we saw that the radiation modes have both incoming and outgoing waves with respect to the vertical direction. However, they do not satisfy the appropriate boundary condition, that is, they should have only the outgoing wave from the slab at $z=\pm\infty$. In order to satisfy this boundary condition we add a negative infinitesimal imaginary part to ω^2 of the radiation mode as $\omega^2\rightarrow\omega^2-i\epsilon$. Since the z component of the wave vector in the upper and lower layers is defined by Eq. (24), k_1 is modified as $k_1\rightarrow k_1-i\epsilon$. This drops the incoming wave of the radiation mode at $z=\pm\infty$. Using this prescription the contribution of the radiation modes in Eq. (11) can be written as

$$-\frac{L}{\pi}\sum_{p=\mathrm{TE,TM}}\int_{c\mathbf{k}_p/\sqrt{\epsilon_1}} d\omega\,\rho(\omega)c^2 \times\left(\frac{P}{\omega^2-\omega_0^2}+i\pi\delta(\omega^2-\omega_0^2)\right) \times\left|\int d^3x\frac{1}{\epsilon_{\mathrm{pe}}(\mathbf{x})}\epsilon_{\mathrm{un}}^2(z)\mathbf{E}_p^{r*}(\mathbf{x})\cdot\mathbf{E}_0(\mathbf{x})\right|^2, \quad (44)$$

where P denotes Cauchy's principal value.

As was mentioned, the factor L coming from the state density of the radiation modes cancels with the factor $1/L$ of the normalization factor of the radiation modes. Thus, the radiation modes give a finite correction to the eigenfrequency in the second order perturbation. In the above expression the term including the principal value gives the real part in Ω_2^2. On the other hand, the term including the δ function gives the imaginary part in Ω_2^2 and causes the appearance of an imaginary part in the eigenfrequency. In contrast to the former term, in the latter term it is sufficient to consider the radiation modes with the same frequency as that of the guided mode in the zeroth order approximation. In fact the latter term has the form of Fermi's golden rule for scattering problems. From this term we can extract properties of the diffraction loss. Strictly speaking, we should treat the diffraction loss as a consequence of the out-of-plane Bragg scattering. In this case a framework that describes scattering processes is needed. However, in such a treatment we cannot appropriately describe the property that the real part of the eigenfrequency forms a band structure. In order to treat both the real and imaginary parts of the eigenfrequency in a unified manner, the authors believe that time-independent perturbation theory with the above prescription is best.

Since the imaginary term vanishes if $\omega_0<c|\mathbf{k}_p|/\sqrt{\epsilon_1}$, it affects only the modes above the light line. This is the origin of the stability of the guided modes, which are defined below the light line. The diffraction loss is quantitatively represented by a quality factor. The quality factor Q is defined by the ratio between the real and imaginary parts of the eigenfrequency Ω. In second order perturbation the quality factor is given by

$$Q=-2\frac{\Omega_0^2}{\mathrm{Im}\,\Omega_2^2}. \quad (45)$$

Let us discuss the consequences of the leaky mode in a transmission measurement. For simplicity, we assume there is only one leaky mode that can be coupled at the boundary with incident light at a given frequency and a given direction of propagation. In this case the attenuation of the optical transmittance is qualitatively estimated by the damping factor

$$\exp\left(-\frac{\mathrm{Re}(\omega)D}{Qv}\right), \quad (46)$$

where v and D are the group velocity of the leaky mode and the thickness of the slab along the propagation direction. Here we emphasize that the quality factor Q comes from the imaginary part of the eigenfrequency of the leaky mode and that the wave number vector is real in our treatment. On the other hand the attenuation of the transmittance is also estimated by a particular eigenvalue of the transfer matrix,[22–25] which describes the scattering processes of a monolayer with the relevant periodicity. An eigenvalue problem of the transfer matrix T is generally written as

$$Tu_n=e^{ik_\perp d}u_n, \quad (47)$$

with the Bloch wave number $k_\perp$ along the propagating direction and the distance d between two adjacent layers. We should note that the frequency and wave number vector parallel to the boundary surface are real quantities in the transfer matrix method. Thus, the Bloch wave number $k_\perp$ becomes complex, because we assume there is no real eigenstate at ω. The so-called complex band structure obtained by Eq. (47) is closely related to our method. In both methods infinite spatial extent is assumed, whereas a kind of energy loss is also taken into account. Since the transmission for l layers is given by a diagonal element of T^l, the attenuation of the transmittance is estimated by

$$\exp(-|\mathrm{Im}\,k_\perp^0|D), \quad D=ld, \quad (48)$$

where $k_\perp^0$ is the Bloch wave number that has the smallest absolute value of the imaginary part in $k_\perp^0$. Thus, the quality factor Q is related to the imaginary part by

$$\frac{1}{Q}=|\mathrm{Im}\,k_\perp^0|\frac{v}{\mathrm{Re}(\omega)}. \quad (49)$$

In the case that there are several leaky modes at a given frequency and a given direction of propagation, the coupling between the bulk eigenmodes and incident light is another important factor in the transmittance. However, it does not depend on the thickness D. Thus, the transmittance is still estimated by Eq. (48), where $k_\perp^0$ is regarded as the complex Bloch wave number of the dominant leaky mode.

As a representative example, we consider the quality factors of the leaky modes in the Γ_1-K_0 interval. As we saw in Sec. IV, the first order perturbation lifts the degeneracy in the modes with different parities of σ_y. The TE (TM) radiation mode has $\sigma_y=-1$ (1) in this interval. Owing to the selection rule, the lifted mode with $\sigma_y=1$ (-1) does not couple to the TE (TM) radiation mode. Since the imaginary part in Ω_2^2 is caused by the radiation mode, it is sufficient to calculate the effects of the radiation modes. The imaginary parts in Ω_2^2 of the lifted modes are given by

$$\mathrm{Im}\frac{\Omega_2^2}{c^2}=-L\rho(\omega_0,\mathbf{k}_p)\frac{4\omega_0[c\epsilon_0\epsilon_2k_2^rS(\widehat{\mathbf{k}_p-\mathbf{G}_{1,0}})_yU_1]^2}{N_{\mathrm{TM}}^r(\omega_0,\mathbf{k}_p)N_{\mathrm{TE}}^g(\omega_0,\mathbf{k}_p-\mathbf{G}_{1,0})} \times\left(\frac{\sin[(k_2^g+k_2^r)d/2]}{2(k_2^g+k_2^r)}+\frac{\sin[(k_2^g-k_2^r)d/2]}{2(k_2^g-k_2^r)}\right)^2 \quad (50)$$

for $\sigma_y=1$ and

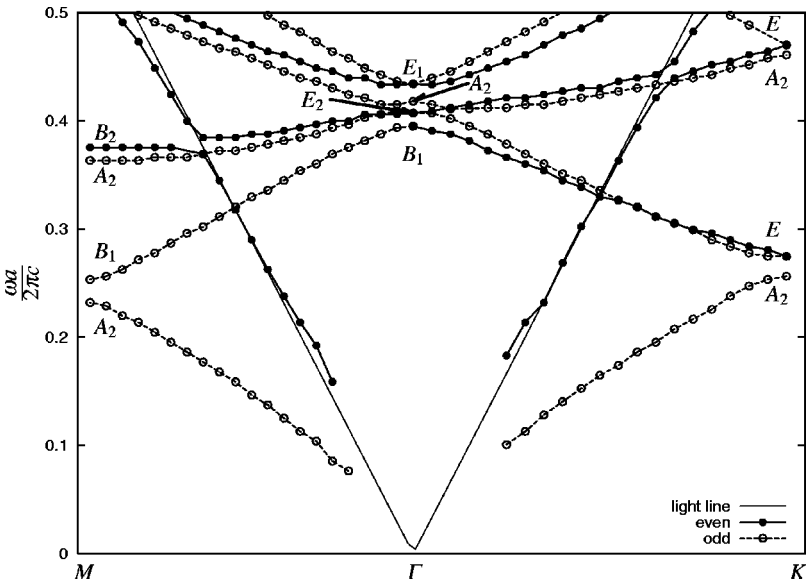

FIG. 4. The band structure of a photonic crystal slab in terms of the FDTD method. The photonic crystal slab consists of a hexagonal array of dielectric cylinders with radius $r=0.25\times a$ and dielectric constant $\epsilon_{\mathrm{rod}}=(2.5)^2$ fabricated on a dielectric slab with thickness $d=0.5\times a$ and dielectric constant $\epsilon_2=(3.4)^2$. The slab is sandwiched by air ($\epsilon_1=1.0$).

$$\mathrm{Im}\frac{\Omega_2^2}{c^2}=-L\rho(\omega_0,\mathbf{k}_p)\frac{4\omega_0^3[c\epsilon_0^2\epsilon_2^2S(\widehat{\mathbf{k}_p-\mathbf{G}}_{1,0})_xU_1]^2}{N_{\mathrm{TE}}^r(\omega_0,\mathbf{k}_p)N_{\mathrm{TE}}^g(\omega_0,\mathbf{k}_p-\mathbf{G}_{1,0})}\times\left(\frac{\sin[(k_2^g+k_2^r)d/2]}{2(k_2^g+k_2^r)}+\frac{\sin[(k_2^g-k_2^r)d/2]}{2(k_2^g-k_2^r)}\right)^2 \tag{51}$$

for $\sigma_y=-1$. Here, k_2^g and k_2^r are defined as

$$k_2^g=\sqrt{\epsilon_2\frac{\omega_0^2}{c^2}-(\mathbf{k}_p-\mathbf{G}_{1,0})^2},$$

$$k_2^r=\sqrt{\epsilon_2\frac{\omega_0^2}{c^2}-\mathbf{k}_p^2}. \tag{52}$$

In the above expressions the singularity in $\rho(\omega_0,\mathbf{k}_p)$ on the light line is canceled by the term proportional to $1/k_1^2$ in the normalization factor of the radiation modes. As a consequence, $\mathrm{Im}\Omega_2^2$ scales as $\sqrt{\epsilon_1\omega_0^2/c^2-\mathbf{k}_p^2}$ near the light line. This implies a rapid increase of the decay rate near the light line as the dispersion curve crosses it. Since the leaky modes other than E_1 are stable at the Γ_1 point, the decay rate or the inverse of the quality factor has a peak in this interval as a function of $\mathbf{k}_p$.

In the Γ_1-K_1 interval $\mathrm{Im}(\Omega_2^2/c^2)$ of the leaky modes can be obtained by replacing the reciprocal lattice vector $\mathbf{G}_{1,0}$ in Eq. (50) and Eq. (51) by $\mathbf{G}_{0,-1}$. As we can see in Fig. 1, $[(\widehat{\mathbf{k}_p-\mathbf{G}}_{0,-1})_x]^2$ is smaller than $[(\widehat{\mathbf{k}_p-\mathbf{G}}_{0,1})_x]^2$ and the difference becomes large if $\mathbf{k}_p$ approaches the origin. Thus, compared with the band in Γ_1-K_0 with $\sigma_y=-1$ stability is expected for the band in Γ_1-K_1 with $\sigma_y=-1$.

V. NUMERICAL CALCULATIONS

Taking account of the analytical results obtained in the previous section, we performed numerical calculations of the band structure for the guided and leaky modes in a photonic crystal slab. We deal with a two-dimensional photonic crystal slab composed of a hexagonal array of dielectric cylinders fabricated in a dielectric slab. The slab is sandwiched by air in the vertical direction. The following parameters were assumed: $d=0.5\times a$, $\epsilon_1=1.0$, $\epsilon_2=(3.4)^2$, $\epsilon_{\mathrm{rod}}=(2.5)^2$, and $r=0.25\times a$. Photonic crystal slabs of this kind have been experimentally fabricated by several groups[5,7] and have been one of the main subjects of recent investigations. Usually the dielectric cylinders are air. However, in this case the periodic modulation is so strong that agreement with the nearly free-photon approximation cannot be expected. Thus, we assumed a rather artificial value for ϵ_{rod}.

We use the FDTD scheme as an *ab initio* method to calculate the band structure. Then, we compare the results obtained by the FDTD method with those of the nearly free-photon approximation. In the FDTD scheme we can treat both real and imaginary parts of the eigenfrequencies. Details of the methodology used in this section are given in our previous paper.[21] In order to calculate the band structure in the FDTD method, the unit cell was divided into $1152(=2\times24^2)$ meshes. Further decrease in the size of the spatial

TABLE I. Comparison of the eigenfrequencies at the Γ, K, and M points. The second, third, and fourth columns show the irreducible representations of corresponding k groups, the real parts of the eigenfrequencies in terms of FDTD, and the real parts of the eigenfrequencies in terms of the nearly free-photon approximation (NFPA).

	k group	IRR	FDTD	NFPA
Γ	C_{6v}	B_1	0.375	0.399
		E_2	0.407	0.417
		A_2	0.418	0.440
		E_1	0.434	0.441
K	C_{3v}	A_2	0.256	0.261
		E	0.275	0.282
M	C_{2v}	A_2	0.232	0.234
		B_1	0.253	0.259

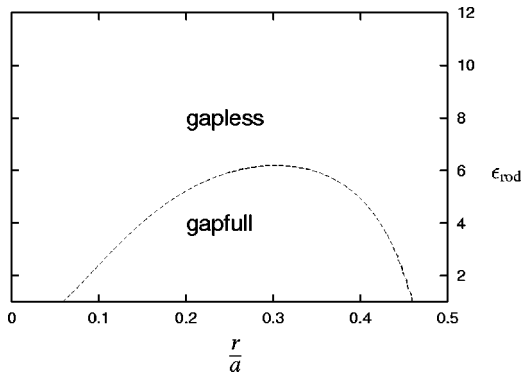

FIG. 5. The phase diagram of the photonic crystal slab showing the photonic band gap between the lowest and second bands in the nearly free-photon approximation. The parameters ϵ_1, ϵ_2, d are the same as those given above. The dashed line is the phase boundary between the gapless and gapfull phases.

mesh did not give an apparent change in the eigenfrequencies.

The photonic band structure in terms of the FDTD method is shown in Fig. 4. The irreducible representations were assigned from numerical results. The band structure has a close resemblance to that of the empty lattice given in Fig. 2. However, the connectivity among the bands is modified. For example, the second even band ($\sigma_y=1$) in the Γ-K interval meets two anticrossings in accordance with the noncrossing rule between bands with the same symmetry. A photonic band gap of the guided modes does not open in this case. This is due to the small periodic modulation.

First, we compare the eigenfrequencies at the Γ, K, and M points. The eigenfrequencies of the modes that correspond to the Γ_1, K_0, and M_0 points in the zeroth order approximation are listed in Table I. The third and fourth columns are the eigenfrequencies in units of $2\pi c/a$ obtained by the FDTD method and by the nearly free-photon approximation. The discrepancy between the FDTD and the nearly free-photon results is within 5% at these points. These results indicate the efficiency of the nearly free-photon approximation.

Next, we consider the photonic band gap below the light line. As was mentioned, a photonic band gap between the lowest and second bands below the light line tends to open in photonic crystal slabs composed of a hexagonal array of cylindrical air holes. However, if the air holes are replaced by other dielectric materials, it is not well known whether the gap opens or not. In order to solve this problem, we estimated the phase boundary between the gapless and gapfull phases in the nearly free-photon approximation. The phase diagram is shown in Fig. 5. Here, ϵ_1, ϵ_2, and d are same as those given above and the phase space is spanned by r and $\epsilon_{\rm rod}$. Below the dashed line a photonic band gap appears in this approximation. Around the lower right corner of the figure the phase boundary is expected to be modified, because in this region the periodic modulation is strong. From this figure we can see that the gap closes if $\epsilon_{\rm rod}>6$ or $r<0.06a$ in this approximation.[26]

The nearly free-photon approximation predicts that the second and third odd bands in the Γ-K interval are almost TE polarized. We checked them by calculating the ratio $\langle E_z^2\rangle/(\langle E_x^2+E_y^2\rangle)$ in terms of the FDTD method. Here, $\langle\cdots\rangle$ denotes the spatial average. For the second and third bands the ratios are less than 0.014 and 0.01, respectively, while their magnetic counterparts $\langle H_z^2\rangle/(\langle H_x^2+H_y^2\rangle)$ are greater than 2.8 and 3.3, respectively. These small values indicate that these band are almost TE polarized.

The decay rates of the second and third odd bands in the Γ-K interval were calculated both by the FDTD method and by Eq. (51) of the nearly free-photon approximation. The results are shown in Fig. 6. As we can see, the nearly free-photon approximation well describes the FDTD results regarding the order of magnitude and the difference between the two bands. Since these bands have the E_2 and A_2 representations at the Γ point, the decay rates should become zero at the Γ point. The results of FDTD calculations show the correct behavior.[27] In terms of Eq. (51) of the nearly free-photon approximation, such behavior cannot be expected.

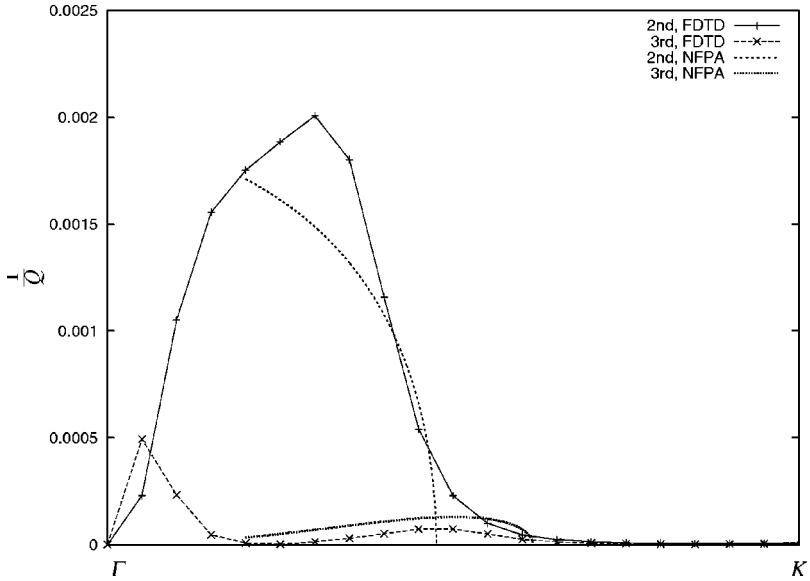

FIG. 6. The decay rates $(1/Q)$ of the second and third odd bands in the Γ-K interval by the FDTD method and by the nearly free-photon approximation.

Near the Γ point, six dispersion curves gather. In Eq. (51) only two degenerate bands in the Γ_1-K_0 interval are taken into account. In order to get correct behavior we must take into account the other four bands near the Γ point. If we do so, we will get well-approximated behavior.

VI. CONCLUSION

In summary, we have studied the nearly free-photon approximation for photonic crystal slabs. The first order perturbation predicts the dominant shift of the real parts of the eigenfrequencies and the irreducible representations of the eigenmodes. The second order perturbation incorporates the imaginary parts of the eigenfrequencies of the leaky modes. The analytical expressions for the eigenfrequencies and the irreducible representations agree quite well with numerical results obtained by the FDTD method.

In this paper we restricted ourselves to symmetric photonic crystal slabs and their even modes with respect to the parity in the vertical direction. However, it is easy to generalize the analytical results to asymmetric photonic crystal slabs and to the odd modes in symmetric photonic crystal slabs. Usually, photonic crystal slabs are fabricated on semiconductor substrates. The air-bridge type, which is considered in the previous section, is not necessarily realistic from this point of view. A photonic crystal slab on a substrate is inevitably asymmetric. If the dielectric constant of the substrate is close to that of the dielectric slab, the region of guided modes becomes narrow in frequency. Thus, the TE and TM modes are almost degenerate in the entire k space. To clarify the band structure of such asymmetric photonic crystal slabs is an important issue for material design.

ACKNOWLEDGMENTS

One of the authors (T.O.) was supported by Project No. IST-1999-19009 PHOBOS of the European Commission. K.S. was supported by the Mitsubishi Foundation.

[1] E. Yablonovitch, Phys. Rev. Lett. **58**, 2059 (1987).
[2] S. John, Phys. Rev. Lett. **58**, 2486 (1987).
[3] See, for example, A. Yariv and P. Yeh, *Optical Waves in Crystals* (Wiley, New York, 1984).
[4] P.L. Gourley, J.R. Wendt, G.A. Vawter, T.M. Brennan, and B.E. Hammons, Appl. Phys. Lett. **64**, 687 (1994).
[5] M. Kanskar, P. Paddon, V. Pacradouni, R. Morin, A. Busch, J.F. Young, S.R. Johnson, J. MacKenzie, and T. Tiedje, Appl. Phys. Lett. **70**, 1438 (1997).
[6] D. Labilloy, H. Benisty, C. Weisbuch, T.F. Krauss, R.M. De La Rue, V. Bardinal, R. Houdre, U. Oesterle, D. Cassagne, and C. Jouanin, Phys. Rev. Lett. **79**, 4147 (1997).
[7] B. D'Urso, O. Painter, J. O'Brien, T. Tombrello, A. Yariv, and A. Scherer, J. Opt. Soc. Am. B **15**, 1155 (1998).
[8] D. Labilloy, H. Benisty, C. Weisbuch, C.J.M. Smith, T.F. Krauss, R. Houdre, and U. Oesterle, Phys. Rev. B **59**, 1649 (1999).
[9] S. Fan, P.R. Villeneuve, J.D. Joannopoulos, and E.F. Schubert, Phys. Rev. Lett. **78**, 3294 (1997).
[10] P.R. Villeneuve, S. Fan, S.G. Johnson, and J.D. Joannopoulos, IEE Proc.: Optoelectron. **145**, 384 (1998).
[11] O. Painter, J. Vuckovic, and A. Scherer, J. Opt. Soc. Am. B **16**, 275 (1999).
[12] J.K. Hwang, H.Y. Ryu, and Y.H. Lee, Phys. Rev. B **60**, 4688 (1999).
[13] S.G. Johnson, S. Fan, P.R. Villeneuve, J.D. Joannopoulos, and L.A. Kolodziejski, Phys. Rev. B **60**, 5751 (1999).
[14] H. Benisty, D. Labilloy, C. Weisbuch, C.J.M. Smith, T.F. Krauss, D. Cassagne, A. Beraud, and C. Jouanin, Appl. Phys. Lett. **76**, 532 (2000).
[15] S. Kuchinsky, D.C. Allan, N.F. Borrelli, and J.C. Cotteverte, Opt. Commun. **175**, 147 (2000).
[16] P. Paddon and J.F. Young, Phys. Rev. B **61**, 2090 (2000).
[17] A. Chutinan and S. Noda, Phys. Rev. B **62**, 4488 (2000).
[18] S.G. Johnson, S. Fan, P.R. Villeneuve, and J.D. Joannopoulos, Phys. Rev. B **62**, 8212 (2000).
[19] D. Cassagne, C. Jouanin, and D. Bertho, Phys. Rev. B **53**, 7134 (1996).
[20] See, for example, N. W. Ashcroft and N. D. Mermin, *Solid State Physics* (Saunders College, Philadelphia, 1976).
[21] T. Ochiai and K. Sakoda, Phys. Rev. B **63**, 125107 (2001).
[22] J.B. Pendry and A. MacKinnon, Phys. Rev. Lett. **69**, 2772 (1992).
[23] N. Stefanou, V. Karathanos, and A. Modinos, J. Phys.: Condens. Matter **4**, 7389 (1992).
[24] Y. Qiu and K.M. Leung, Proc. SPIE **2117**, 32 (1994).
[25] K. Ohtaka, T. Ueta, and K. Amemiya, Phys. Rev. B **57**, 2550 (1998).
[26] We should note that the phase diagram can be calculated more accurately by the FDTD method or by the supercell method in the plane wave expansion.
[27] The peak near Γ of the third band in terms of FDTD is related to the unstable E_1 mode at Γ.